Proceedings of the Symposium A of the European Materials Research, Warsaw, September 2008

Effect of Fe^{2+} (Fe^{3+}) Doping on Structural Properties of CeO_2 Nanocrystals

M. Radović[a], Z. Dohčević-Mitrović[a,*], N. Paunović[a], M. Šćepanović[a], B. Matović[b] and Z.V. Popović[a]

[a]Center for Solid State Physics and New Materials, Institute of Physics, Belgrade, Serbia

[b]Institute of Nuclear Sciences "Vinča", 11001 Belgrade, Serbia

We have measured the Raman scattering and magnetization of pure and Fe^{2+}(Fe^{3+}) doped CeO_2 nanopowders at room temperature. The Raman scattering spectra revealed the existence of CeO_2 fluorite cubic structure for all investigated samples. The Raman active mode at about 600 cm^{-1}, seen in all samples, can be ascribed to the CeO_2 intrinsic oxygen vacancies. Additional Raman modes at 720 cm^{-1}, 1320 cm^{-1} and 1600 cm^{-1}, which appear in the spectra of doped samples, can be assigned to maghemite (γ-Fe_2O_3) cation deficient structure, to $2\omega_{LO}$ IR-allowed overtone and two magnon structure, respectively. This implies that our powders are composed of mixed valence states and have defective structure. Presence of oxygen defect states and magnetic ions can be responsible for the observed ferromagnetism at room temperature in both pure and Fe doped samples.

PACS numbers: 61.72.uj, 78.30.−j, 75.50.Tt

1. Introduction

Nanostructured CeO_2 based materials have reached significant impact in practical applications due to general improvement of catalytic [1], electrical [2], optical [3] and electrooptical [4] properties. Technology of solid oxide fuel cells is currently the most relevant field where CeO_2 found applications [5].

Various methods of preparation, such as sol-gel [4], spray pyrolysis [6], sputtering [3], have been used to obtain nanosized CeO_2. One of the major challenges for the preparation of these nanostructured oxides is precise control of particle size. In our recent studies [7–9], nanoparticles of CeO_2 doped with Nd, Y, and Ba were prepared with self propagating room temperature (SPRT) synthesis. With this cost and time effective method we were able to produce nanocrystalline materials with an average particle size below 10 nm. CeO_2 nanocrystals doped with 3*d* elements such as Fe, were obtained for the first time by this method of preparation.

Vibrational properties of nanocrystalline systems are dependent on the reduction of crystallite size. Room temperature Raman scattering measurements of CeO_2 nanoparticles revealed that the energy of the F_{2g} Raman active mode decreases and the line width increases followed by an asymmetrical broadening with decreasing particle size [10]. Several factors as inhomogeneous strain, phonon confinement, particle size distribution and the presence of defect states were considered to explain such changes [7].

* corresponding author; e-mail: zordoh@phy.bg.ac.yu

The magnetic properties of CeO_2 nanocrystals have been the subject of several studies [11, 12]. The existence of room temperature ferromagnetism in CeO_2 nanoparticles is discovered recently whereas bulk counterpart are diamagnetic. It is assumed that the origin of ferromagnetism may be the exchange interactions between unpaired electron spins arising from oxygen vacancies presented at the surfaces of nanoparticles [11].

In the present work, we used Raman scattering and magnetic measurements to determine the effect of Fe^{2+} and Fe^{3+} doping on structural and magnetic properties of CeO_2 nanocrystals.

2. Experiment

Nanocrystalline $Ce_{1-x}Fe_x^{2+}(Fe_x^{3+})O_{2-y}$ ($x = 0.12$ and 0.06) samples were prepared by the SPRT synthesis using metal nitrates and sodium hydroxide as the starting materials. The synthesis involves hand-mixing of starting materials in alumina mortar for 5–7 min until the mixture gets light brown. After being exposed to air for three hours, the mixture was suspended in water. Rinsing out of reaction byproduct ($NaNO_3$) was performed by centrifuge Centurion 1020D at 3500 rpm. This procedure was performed three times with distilled water and twice with ethanol. The Fe^{2+} doped solid-state solution was obtained according to reaction

$$2[(0.88)Ce(NO_3)_3 \cdot 6H_2O + (0.12)FeNO_3] + 6NaOH + (1/y)O_2 \rightarrow 2Ce_{0.88}Fe_{0.12}O_{2-y} + 6NaNO_3 + 9H_2O, \quad (1)$$

whereas Fe^{3+} doped solid state solution was obtained according to reaction

$$2[(0.88)Ce(NO_3)_3 \cdot 6H_2O + (0.12)Fe(NO_3)_3 \cdot 6H_2O] + 6NaOH + (1/2 - y)O_2 \rightarrow 2Ce_{0.88}Fe_{0.12}O_{2-y} + 6NaNO_3 + 15H_2O. \quad (2)$$

Unpolarized Raman scattering measurements were performed in the backscattering configuration using micro-Raman Jobin Yvon T64000 system. As an excitation source 514.5 nm line of Ar^+ laser was used. In order to avoid sample heating we used very low laser power on the sample (0.24 mW).

Magnetic moment measurements at room temperature were performed using vibrating sample magnetometer (VSM 200) of 14 T cryogen free measurement system (Cryogenic Ltd.).

3. Results and discussion

In Fig. 1 we present room temperature Raman spectra of the $Ce_{1-x}Fe_x^{2+}(Fe_x^{3+})O_{2-y}$ ($x = 0.12$ and 0.06) samples together with the Raman spectrum of pure nanocrystalline CeO_2 sample. The first order F_{2g} Raman active mode of CeO_2 nanocrystals appears at 454 cm^{-1}. Besides the F_{2g} mode there are additional modes at 600 cm^{-1} and 1048 cm^{-1} which are assigned to intrinsic oxygen vacancies (V_{Ce3+}) [7] and the second order Raman mode at X-point of the Brillouin zone [13], respectively.

In the Raman spectrum of Fe^{2+} doped sample ($Ce_{0.88}Fe_{0.12}^{2+}O_{2-y}$), the F_{2g} mode is located at nearly the same frequency as the F_{2g} mode of pure CeO_2 nanocrystalline sample, with slightly increased line width. Beside the F_{2g} and oxygen vacancy modes, a weak band appears at 720 cm^{-1} (marked with * in Fig. 1), which is assigned to maghemite (γ-Fe_2O_3) cation deficient structure [14]. $2\omega_{LO}$ (IR-active) overtone, characteristic for hematite (α-Fe_2O_3), appears at 1320 cm^{-1} [14]. The appearance of modes characteristic for different iron oxide crystal structures can be a consequence of oxidation of mixed valence iron oxide (magnetite Fe_3O_4), probably caused by laser irradiation.

In the Raman spectrum of Fe^{3+} doped sample ($Ce_{0.88}Fe_{0.12}^{3+}O_{2-y}$), the F_{2g} mode is shifted to lower energies and is broader than in the spectra of pure, Fe^{2+} and Fe^{2+}/Fe^{3+} ceria doped samples. Red shift and broadening of the F_{2g} mode can be ascribed to the size and strain effects [7, 10] or can be a consequence of electron molecular vibrational coupling due to the increased concentration of defects in oxygen sub-lattice of CeO_2 and presence of magnetic ions in ceria lattice.

The intensity of intrinsic oxygen vacancy Raman active mode (V_{Ce3+}) in $Ce_{0.88}Fe_{0.12}^{3+}O_{2-y}$ sample is more pronounced than in other samples. Such behavior confirms our previous statement that incorporation of trivalent iron in ceria lattice provokes a formation of more defective structure, i.e. higher concentration of oxygen vacancies is formed with Fe^{3+} doping. The Raman active mode at 1320 cm^{-1} can be assigned to $2\omega_{LO}$ IR-allowed overtone of Fe_2O_3, whereas a weak structure at about 1600 cm^{-1} can be ascribed to two-magnon peak of Fe_2O_3 phase [14].

In Fig. 1 there are also shown the Raman spectra of mixed valence Fe-doped ceria sample ($Ce_{0.88}Fe_{0.06}^{2+}Fe_{0.06}^{3+}O_{2-y}$). The frequency of the F_{2g} mode, for this sample, lies between the F_{2g} values for Fe^{2+} and Fe^{3+} doped samples. The intensity of $2\omega_{LO}$ IR-allowed overtone and two magnon mode of Fe_2O_3 in this sample is significantly higher than in ($Ce_{0.88}Fe_{0.12}^{3+}O_{2-y}$) sample. The appearance of iron oxide Raman modes implies high structural disorder in this sample.

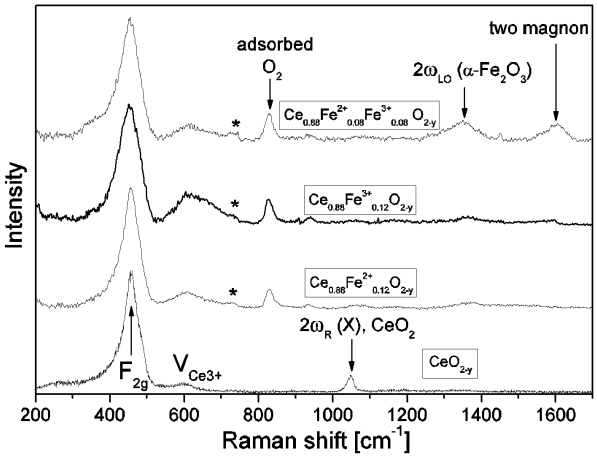

Fig. 1. Room temperature Raman spectra of Fe^{2+}/Fe^{3+} doped and pure CeO_2 nanocrystalline samples.

Interesting feature in the Raman spectra of all doped samples, is a mode located at about 830 cm^{-1}, which is not observed in the spectra of pure CeO_2. This mode is characteristic for adsorbed oxygen species on the surface of CeO_2 nanoparticles [15] suggesting that doping with iron can lead to better chemical activity of ceria nanoparticles.

In Fig. 2 there is shown magnetization versus magnetic field for polycrystalline and nanocrystalline CeO_2 samples, measured at 300 K. The bulk sample shows a weak diamagnetic response, as it can be expected for CeO_2 with Ce^{4+} ions in the $4f^0$ electronic configuration. On the other hand, CeO_2 nanocrystals show weak ferromagnetic behavior. It has been observed that nonmagnetic oxides at room temperature become weakly ferromagnetic when the samples are in the form of small nanoparticles [11, 12] or very thin films [16].

It was suggested that the origin of this ferromagnetism may be exchange interaction between unpaired electron spins arising from oxygen vacancies formed at surface of nanoparticles [16, 11]. We believe that $4f^1$ unpaired electron spins in Ce^{3+}, formed at nanoparticles surface, are responsible for room temperature ferromagnetism in nano CeO_2. Saturation magnetization of our CeO_2 nanocrystals is about 0.0055 emu/g which is comparable with previous results [11, 12].

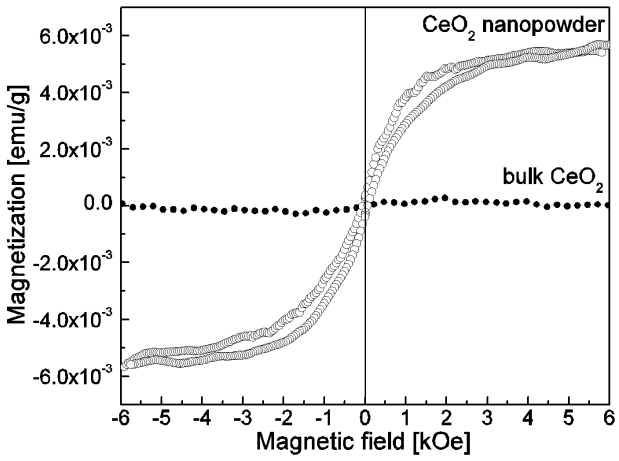

Fig. 2. Room temperature magnetization versus magnetic field for bulk and nanopowdered CeO_2 samples.

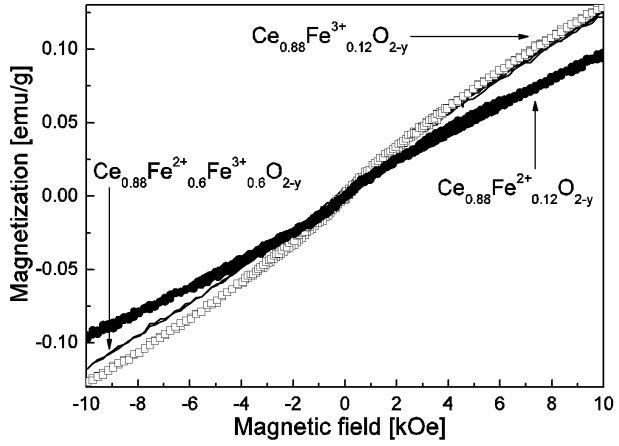

Fig. 3. Magnetization versus magnetic field for the $Ce_{1-x}Fe_x^{2+}(Fe_x^{3+})O_{2-y}$ ($x = 0.12$ and 0.06) samples measured at 300 K.

In Fig. 3 there is shown magnetization versus magnetic field for the $Ce_{1-x}Fe_x^{2+}(Fe_x^{3+})O_{2-y}$ ($x = 0.12$, 0.06) samples, measured at 300 K. It can be seen that Fe-doped CeO_2 samples show paramagnetic response with small ferromagnetic component in these samples.

The ferromagnetic component only, obtained by subtracting the linear paramagnetic background from $M(H)$ curves in Fig. 3 is given in Fig. 4. The hysteresis loop for the Fe^{2+}/Fe^{3+} doped sample (Fig. 4) is between the loops for Fe^{2+} and Fe^{3+} doped samples. Saturation magnetizations (at 10 kOe) can be roughly estimated to be 0.009, 0.014 and 0.018 emu/g for the Fe^{2+}, Fe^{2+}/Fe^{3+} and Fe^{3+} doped samples, respectively.

This means that the value of saturation magnetization for the sample doped with Fe^{2+}, Fe^{3+} is roughly in the middle between the values of saturation magnetization for Fe^{2+} and Fe^{3+} doped samples, i.e. saturation magnetization of this ferromagnetic component increases with the increase of oxidation state of Fe dopant.

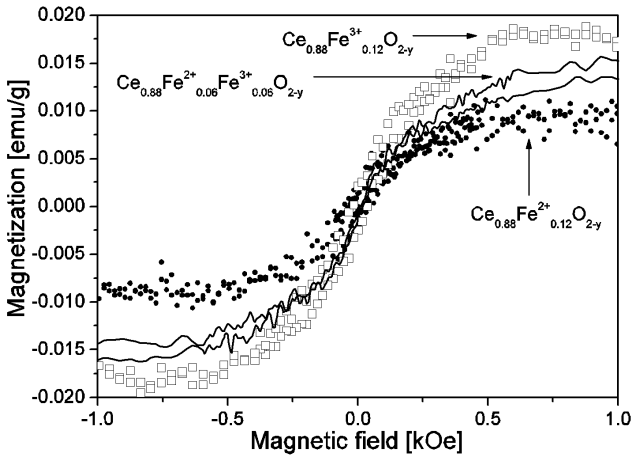

Fig. 4. Hysteresis loops for the $Ce_{1-x}Fe_x^{2+}(Fe_x^{3+})O_{2-y}$ ($x = 0.12$ and 0.06) samples measured at 300 K.

As we already mentioned the existence of Ce^{3+} states may be the origin of room temperature ferromagnetism in nano CeO_2. The exchange interaction between $4f^1$ nonpaired electrons in Ce^{3+} can result in weak ferromagnetism experimentally found in nano CeO_2 (see Fig. 2). By doping with Fe we can expect different behavior in the case of 2+ and 3+ valence state. Iron has $3d^6 + 4s^2$ valence electrons. In the case of low spin state of Fe^{2+} ions all $3d^6$ ions are compensated ($\uparrow\downarrow\uparrow\downarrow\uparrow\downarrow$, $S = 0$) and they do not contribute to the total magnetic moment of nanoceria. In this case iron as dopant produces higher disorder in ceria structure i.e. an increase of oxygen vacancy concentration which further increases the Ce^{3+} ion concentration. In this way, the ferromagnetic exchange interaction is also stronger and magnetization saturation value in Fe^{2+} doped sample is a little bit higher than in pure nano CeO_2 (see Fig. 2 and Fig. 4). In Fe^{3+} doped samples, $3d^5$ electrons in the low spin state can participate in ferromagnetic ordering ($\uparrow\downarrow\uparrow\downarrow\uparrow$, $S = 1/2$). In this case, both Fe^{3+} and Ce^{3+} electron spins contribute to ferromagnetic ordering. Consequently, we can expect dramatic increase in magnetization of Fe^{3+} doped sample, which is experimentally observed in Figs. 3 and 4. In such a way we concluded that the existence of both Ce^{3+}–oxygen vacancies complexes and Fe^{3+} ions in the low spin state contribute to the weak ferromagnetism in nanoceria and not only oxygen vacancies as previously stated [11, 16].

4. Conclusion

Nanocrystalline $Ce_{1-x}Fe_x^{2+}(Fe_x^{3+})O_{2-y}$ ($x = 0.12$ and 0.06) samples were synthesized by self propagating room temperature synthesis method. Raman spectroscopy at room temperature was applied to determine the influence of Fe^{2+}/Fe^{3+} doping on structural and vibrational properties of cerium dioxide nanopowders. Doping with trivalent iron causes redshift and broadening of the F_{2g} mode

as a consequence of electron molecular vibrational coupling due to the increased concentration of Ce^{3+}–oxygen vacancies complexes and magnetic Fe^{3+} ions. The existence of second order Raman modes characteristic for iron oxide suggest that there is a high structural disorder in our samples. From magnetic measurements it was established that nanocrystalline CeO_2 sample exhibit ferromagnetic behavior at room temperature. The Fe-doped ceria samples also exhibit small ferromagnetism at room temperature. The saturation magnetization in all doped samples is higher than in pure ceria and increases with an increase of oxidation state of Fe dopant. The presence of Ce^{3+} and Fe^{3+} spin electrons is responsible for observed ferromagnetism.

Acknowledgments

This work was supported by the Ministry of Science and Technological Development of Republic of Serbia under the project No. 141047, the OPSA-026283 project within the EC FP6 Programme and SASA project F-134.

References

[1] T. Masui, T. Ozaki, K. Machida, G. Adachi, *J. Alloys Comp.* **303**, 49 (2000).

[2] Y.-M. Chiang, E.B. Lavik, I. Kosacki, H.L. Tuller, J.Y. Ying, *Appl. Phys. Lett.* **69**, 8 (1996).

[3] S. Guo, H. Arwin, S.N. Jacobsen, K. Järrendahl, U. Helmersson, *J. Appl. Phys.* **77**, 5369 (1995).

[4] N. Ozer, *Sol. Energy Mater. Sol. Cells* **68**, 391 (2001).

[5] B.C.H. Steele, *Solid State Ionics* **129**, 95 (2000).

[6] J.L.M. Rupp, A. Infortuna, L.J. Gauckler, *Acta Mater.* **54**, 1721 (2006).

[7] Z.D. Dohčević-Mitrović, M.J. Šćepanović, M.U. Grujić-Brojčin, Z.V. Popović, S.B. Bošković, B.M. Matović, M.V. Zinkevich, F. Aldinger, *Solid State Commun.* **137**, 387 (2006).

[8] Z.D. Dohčević-Mitrović, M. Grujić-Brojčin, M. Šćepanović, Z.V. Popović, S. Bošković, B. Matović, M. Zinkevich, F. Aldinger, *J. Phys., Condens. Matter* **18**, 1 (2006).

[9] M. Radović, Z.D. Dohčević-Mitrović, M. Šćepanović, M. Grujić-Brojčin, B. Matović, S. Bošković, Z.V. Popović, *Sci. Sinter.* **39**, 281 (2007).

[10] J.E. Spanier, R.D. Robinson, F. Zhang, S.W. Chan, I.P. Herman, *Phys. Rev. B* **64**, 245407 (2001).

[11] A. Sundaresan, R. Bhargavi, N. Rangarajan, U. Siddesh, C.N.R. Rao, *Phys. Rev. B* **74**, 161306(R) (2006).

[12] Y. Liu, Z. Lockman, A. Aziz, J. MacManus-Driscoll, *J. Phys., Condens. Matter* **20**, 165201 (2008).

[13] G.A. Kourouklis, A. Jayaraman, G.P. Espinosa, *Phys. Rev. B* **37**, 4250 (1988).

[14] M.J. Massey, U. Baier, R. Merlin, W.H. Weber, *Phys. Rev. B* **41**, 7822 (1990).

[15] Y.M. Choi, H. Abernathy, H.T. Chen, M.C. Lin, M. Liu, *Chem. Phys. Chem.* **7**, 1957 (2006).

[16] M. Venkatesan, C.B. Fitzgerald, J.M.D. Coey, *Nature* **430**, 630 (2004).